Available online at www.sciencedirect.com
ScienceDirect
Mathematical Biosciences 206 (2007) 61–80
Mathematical Biosciences
www.elsevier.com/locate/mbs

A diffusive SI model with Allee effect and application to FIV

Frank M. Hilker [a,b,*], Michel Langlais [c], Sergei V. Petrovskii [d], Horst Malchow [a]

[a] *Institute of Environmental Systems Research, Department of Mathematics and Computer Science, University of Osnabrück, 49069 Osnabrück, Germany*
[b] *Gulbenkian Institute of Science, Theoretical Epidemiology Group, Apartado 14, 2781-901 Oeiras, Portugal*
[c] *UMR CNRS 5466, Mathématiques Appliquées de Bordeaux, Case 26, Université Victor Segalen Bordeaux 2, 146 rue Léo-Saignat, 33076 Bordeaux Cedex, France*
[d] *Shirshov Institute of Oceanology, Russian Academy of Science, Nakhimovsky Prospekt 36, Moscow 117218, Russia*

Received 31 March 2004; received in revised form 9 August 2005; accepted 4 October 2005
Available online 4 January 2006

Abstract

A minimal reaction–diffusion model for the spatiotemporal spread of an infectious disease is considered. The model is motivated by the Feline Immunodeficiency Virus (FIV) which causes AIDS in cat populations. Because the infected period is long compared with the lifespan, the model incorporates the host population growth. Two different types are considered: logistic growth and growth with a strong Allee effect. In the model with logistic growth, the introduced disease propagates in form of a travelling infection wave with a constant asymptotic rate of spread. In the model with Allee effect the spatiotemporal dynamics are more complicated and the disease has considerable impact on the host population spread. Most importantly, there are waves of extinction, which arise when the disease is introduced in the wake of the invading host population. These waves of extinction destabilize locally stable endemic coexistence states. Moreover, spatially restricted epidemics are possible as well as travelling infection pulses that correspond either to fatal epidemics with succeeding host population extinction or to epidemics with recovery of the host population. Generally, the Allee effect induces minimum viable population sizes and critical spatial lengths of the initial distribution. The local stability analysis yields bistability and the phenomenon of transient epidemics within the regime of disease-induced extinction. Sustained oscillations do not exist.

* Corresponding author. Address: Gulbenkian Institute of Science, Theoretical Epidemiology Group, Apartado 14, 2781-901 Oeiras, Portugal. Tel.: +351 21 446 4649; fax: +351 21 440 7973.
E-mail address: fhilker@uos.de (F.M. Hilker).

0025-5564/$ - see front matter © 2005 Elsevier Inc. All rights reserved.
doi:10.1016/j.mbs.2005.10.003

Keywords: Epidemiology; SI model; Allee effect; Bistability; Reaction–diffusion system; Travelling waves; Spatial spread

1. Introduction

There is an ongoing interest in the dynamics of infectious diseases and their spatiotemporal spread. Simple compartmental models have been used to understand the principal mechanisms governing disease transmission and have been extended to reaction–diffusion equations to estimate the asymptotic rate of spatial spread [1–6]. For diseases with long incubation and infectivity times, the host population's vital dynamics, i.e., birth and death rates, have to be taken into account. This has been shown to qualitatively change the system behaviour. While in the classic Kermack and McKendrick model [7] the disease dies out or becomes endemic if the basic reproductive ratio is less or greater than one, respectively, the infection can also become endemic in models incorporating vital dynamics [8,9]. If the disease additionally reduces the population size, one has to consider epidemiological models with varying population sizes [10–18]. This may lead in particular cases to a destabilization of the endemic state and to sustained limit cycle oscillations, as has been numerically observed for the first time by Anderson et al. [19].

The aim of this paper is to explore the consequences of different vital dynamics on the disease transmission as well as on the spatial spread. The starting point is an SI model with logistic growth, the standard incidence (also called proportionate mixing or frequency-dependent transmission) and no vertical transmission, which has been proposed and applied by Courchamp et al. [20] to the circulation of the Feline Immunodeficiency Virus (FIV) within domestic cats (*Felis catus*, L.). FIV is a lentivirus which is structurally similar to the Human Immunodeficiency Virus (HIV) and induces feline AIDS (Acquired Immunodeficiency Syndrome) in cats.

The vital dynamics are generalized to be governed by a strong Allee effect. This can be caused by difficulties in finding mating partners at small densities, genetic inbreeding, demographic stochasticity or a reduction in cooperative interactions, see [21–24]. It should be noted, moreover, that the study of Allee dynamics is justified in its own rights, because this is largely lacking in the epidemiological literature, but see [25,26].

The spatial propagation of diseases has been investigated in the literature mainly by way of travelling wave approaches and by approximating the asymptotic rate of spread [27–37]. Two different scenarios will be considered in this study for both the models with logistic growth and Allee effect: On the one hand the spread of infection in a disease-free population which has settled down at carrying capacity in all the space and on the other hand the case that the host population itself still invades into empty space with the disease introduced in the wake of this invasion front. The latter case is of special interest, since the domestic cat is a very opportunistic predator and considered to be one of the worst invasive species threatening many indigenous species around the world. Therefore, FIV has been proposed as biological control method [38,39].

This paper is outlined as follows. In the next section, the basic SI model is described. Then, the results of a detailed local stability analysis of the model with a generalized strong Allee effect are presented. The spatiotemporal spread is studied by numerical simulations and travelling wave approaches in Section 4. Finally, the results are discussed and related to similar work.

2. Model description

Let $P = P(t, \boldsymbol{x}) \geqslant 0$ be the density of the host population (in number of individuals per km^2) at time t (years) and spatial location $\boldsymbol{x}$ (in km). The fertility function $\beta(P) \geqslant 0$ and the mortality function $\mu(P) \geqslant 0$ are assumed to be density-dependent. Then the intrinsic per-capita growth rate is

$$g(P) = \beta(P) - \mu(P).$$

The total population is split into a susceptible part $S = S(t, \boldsymbol{x})$ and an infected part $I = I(t, \boldsymbol{x})$:

$$P = S + I.$$

The disease transmission is assumed to be frequency-dependent; it occurs via proportionate mixing transmission [40–42], i.e., the number of contacts between infected and susceptible individuals is constant, as it has been argued for rural/suburban cat populations [43]. The transmission coefficient is $\sigma > 0$ (per year). In contrast to HIV, the disease is assumed not to be transmitted to offspring. Hence, newborns of the infected are in the susceptible class. The infected suffer an additional disease-related mortality $\alpha > 0$ (per year), which shall be referred to as virulence. There is no recovery from the disease. Removal of infected is only by death. The corresponding transfer diagram is

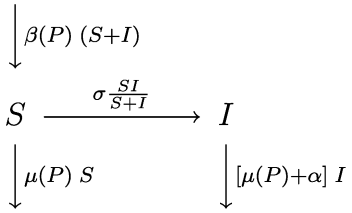

The spatial propagation of the individuals is modelled by diffusion with diffusion coefficients $D_S \geqslant 0$ and $D_I \geqslant 0$ (km^2 per year) for the susceptibles and infected, respectively. This basic model is described by a system of two partial differential equations:

$$\frac{\partial S}{\partial t} = -\sigma \frac{SI}{P} + \beta(P)P - \mu(P)S + D_S \Delta S, \tag{1}$$

$$\frac{\partial I}{\partial t} = +\sigma \frac{SI}{P} - \alpha I - \mu(P)I + D_I \Delta I, \tag{2}$$

where Δ is the Laplacian. The initial and boundary conditions will be specified later.

System (1,2) is an extension of the model by Courchamp et al. [20], which describes the transmission of FIV for the special case of a spatially homogeneous population with $D_S = D_I = 0$ and with logistic growth of the host population, i.e.,

$$\beta(P) = b > 0, \tag{3}$$

$$\mu(P) = m + \frac{r}{K}P, \quad r = b - m, \ \ m > 0, \tag{4}$$

which yields the well-known linearly decreasing per-capita growth rate

$$g(P) = r(1 - P/K).$$

Gao and Hethcote [15] studied SIRS models with density-dependent birth and death rates. The above FIV model is a special case, for which they provided global stability results. Zhou and Hethcote [17] moreover obtained global stability results for a model with generalized logistic growth. If

$$\beta(P) \text{ is non-increasing,} \tag{5}$$

$$\mu(P) \text{ is non-decreasing and} \tag{6}$$

$$g(P) = 0 \text{ has a unique positive solution } K, \tag{7}$$

then the per-capita growth rate $g(P)$ is non-increasing, and K (the carrying capacity) is the unique stationary state of the disease-free, local model, which is globally asymptotically stable for $P(0) > 0$. The SI model with both logistic and generalized logistic growth has four stationary states and exhibits three different dynamics: eradication of the disease, emergence of a stable endemic stationary state or extinction of the host population. Periodic solutions do not exist, which has been proven with the Dulac criterion.

Next, a generalized strong Allee effect in the vital dynamics is considered, which is based upon the assumptions

$$\frac{\mathrm{d}}{\mathrm{d}P} g(P) \begin{cases} > 0 & \text{for } 0 < P < P_{\mathrm{opt}}, \\ < 0 & \text{for } P_{\mathrm{opt}} < P, \end{cases} \tag{8}$$

$$g(P) = 0 \text{ has two positive roots } K_- \text{ and } K_+, 0 < K_- < P_{\mathrm{opt}} < K_+. \tag{9}$$

This yields a per-capita growth rate that is maximal at some intermediate density P_{opt}. The disease-free, local model has three non-negative stationary states: K_- is unstable, K_+ is globally stable in the range $P(0) > P_{\mathrm{opt}}$ while 0 is stable in the range $0 < P(0) < P_{\mathrm{opt}}$. Furthermore, the following assumptions are posed:

$$\beta(P) \text{ is concave in } (0, K_+), \tag{10}$$

$$\mu(P) \text{ is non-decreasing and convex in } (0, K_+), \tag{11}$$

which imply that $g(P)$ is concave.

As a motivating example of the strong Allee effect, the following per-capita growth rate is considered:

$$g(P) = a(K_+ - P)(P - K_-),$$

which is quadratic with $P_{\mathrm{opt}} = (K_+ + K_-)/2$. The parameter $a > 0$ scales the maximum per-capita growth rate. The fertility and mortality functions take the parametric forms

$$\beta(P) = \begin{cases} a(-P^2 + [K_+ + K_- + e]P + c) & \text{for } 0 \leqslant P \leqslant K_+ + K_-, \\ \text{non-negative and non-increasing} & \text{otherwise,} \end{cases} \tag{12}$$

$$\mu(P) = a(eP + K_+K_- + c). \tag{13}$$

The case differentiation in (12) is necessary, because the first case becomes negative for $P > K_+ + K_- + e$. We want to emphasize, that the first case is sufficient for the model analysis provided that the initial conditions are appropriate, e.g. $P \leqslant K_+$. For biological reasons, however, we require for $P > K_+ + K_-$ that the fertility function remains non-negative, non-increasing as

well as continuous. The mortality function linearly increases with P analogously to the logistic behaviour. The fertility function differs in being quadratic. It increases with P for small population densities, reaches a maximum at some intermediate population density and decreases with P for large population densities. The parameters e, $c \geqslant 0$ determine the effect of density-dependence and -independence, respectively. They do not affect, however, the intrinsic per-capita growth rate $g(P)$.

2.1. Parameter values

The parameter values are chosen as follows. The virulence $\alpha = 0.2\ \text{year}^{-1}$ is kept constant as in Courchamp et al. [20]. In the same study, the transmission coefficient has been estimated to be approximately $\sigma = 3.0\ \text{year}^{-1}$. FIV is mainly transmitted through bites during aggressive contacts between cats. Hence, σ is related to the number of contacts between susceptibles and infected resulting in bites and eventually in virus transmission. Since there might be a large variation in the transmission coefficient, we will use σ in the following as bifurcation parameter. The parameters describing the logistic growth are $b = 2.4\ \text{year}^{-1}$, $m = 0.6\ \text{year}^{-1}$ and $K = 200$ individuals per km^2 for rural cat populations, cf. [20]. The resulting fertility and mortality functions are shown in Fig. 1(a). In the Allee effect model, parameterization is more difficult. First of all, $K_+ = 200$ individuals per km^2 is set to the same carrying capacity. Next, let us assume that there is an Allee threshold of ten percent, i.e., $K_- = 20$ individuals per km^2. The remaining parameters are chosen to yield (i) a similar natural mortality function as in the logistic model and (ii) a reduction in the fertility function with decreasing density, cf. Fig. 1(b). The population growth rate exhibiting a

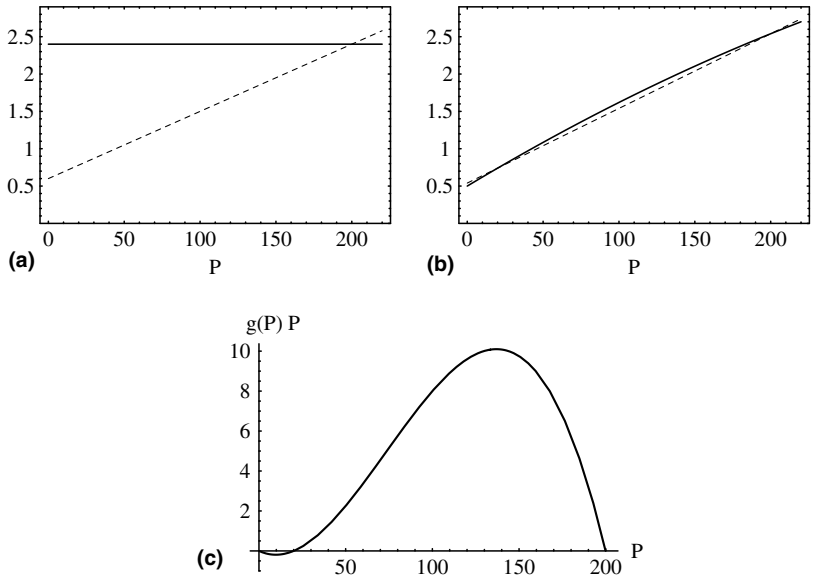

Fig. 1. Fertility function $\beta(P)$ (solid lines) and mortality function $\mu(p)$ (dashed lines) of the models with (a) logistic growth and (b) a strong Allee effect. (c) Population growth rate $g(P) = \beta(P) - \mu(P)$ exhibiting a strong Allee effect. Parameters: $K = K_+ = 200$, $b = 2.4$, $m = 0.6$, $K_- = 20$, $a = 10^{-5}$, $c = 5 \times 10^4$, $e = 10^3$.

strong Allee effect is plotted in Fig. 1(c). Lastly, the diffusion coefficient has to be estimated. The relevant mechanism for population spread is considered to be dispersal [44], since male individuals move under the pressure of dominant males from their native home range to vacant areas. Home range sizes vary from approximately 1 ha for urban stray cats to several hundred ha for populations in non-anthropized habitats, e.g. [43]. Let us assume an observed mean net displacement of 1.77 km for populations of feral domestic cats in rural/suburban areas – having in mind a mean home range of 10 ha and that a dispersing individual has to pass on average five other home ranges before finding a vacant one. Then we can estimate a diffusivity of $D = 1\ \mathrm{km}^2$ per year, cf. Eq. (3.6) in [1]. Naturally, this is a very rough approximation, but the main aim is to explore possible patterns of spatiotemporal dynamics. Though we have the epizootiological problem of FIV spread in mind, we will keep throughout this paper the standard epidemiological notation such as *endemic* instead of *enzootic*, because the investigated model is rather general.

3. Stability results of the non-spatial model with Allee effect

In this section, the existence of the stationary states as well as their stability are summarized for the spatially homogeneous system with assumptions (8)–(11) for a generalized strong Allee effect. Details of the calculations can be found in Appendix A. System (1), (2) with $D_S = D_I = 0$ exhibits a singularity in the transmission term. Introducing the prevalence $i = I/P \in [0, 1]$ and reformulation in (P, i) state variables simplify matters:

$$\frac{\mathrm{d}P}{\mathrm{d}t} = [g(P) - \alpha i]P, \tag{14}$$

$$\frac{\mathrm{d}i}{\mathrm{d}t} = [\sigma - \alpha - \beta(P) - (\sigma - \alpha)i]i. \tag{15}$$

There are six stationary states. They are summarized along with the stability results in Table 1. For the sake of comparison, the stability results of the generalized logistic model are given in Table 2 as well. The formulation in (P, i) state variables allows to distinguish between the trivial extinction state $(0, 0)$ and the disease-induced extinction state $(0, i_2)$ with an ultimate prevalence $i_2 > 0$. The latter one reflects that in the limit process $P \to 0$ there is a non-zero ultimate prevalence, and that the host population goes extinct as a consequence of infection with the disease [45]. The stationary state $(K_+, 0)$ corresponds to the eradication of the disease, so that the disease-free population can settle down at its own carrying capacity. There are two equilibria, which do not exist in the logistic model. First, $(K_-, 0)$, which corresponds to the minimum viable population density in the disease-free Allee model, is always unstable. Second, there is an additional non-trivial stationary state. Denoting the larger and the smaller total population density with P_{3+} and P_{3-}, respectively, there are the non-trivial states (P_{3+}, i_{3+}) and (P_{3-}, i_{3-}).

One of the main results is that, again, sustained periodic oscillations are not possible in the generalized Allee effect model with proportionate mixing transmission. This follows from index theory and the fact that the only unstable interior equilibrium (P_{3-}, i_{3-}), around which a limit cycle could exist, is always saddle, cf. Appendix A.

It should be noted, that as soon as the initial total population verifies $P(0) < K_-$, it follows from (8) and (9) that the population goes extinct, i.e., $P(t) \to 0$ as $t \to \infty$; this dynamics is driven by the

Table 1
Results of the stability analysis of the non-spatial system (14), (15) with generalized Allee effect (8)–(11)

	$\beta(0)$	$\beta(K_-)$		$\beta(K_+)$	
				(*)	$\sigma-\alpha$
$(0,0)$	l.a.s.	unstable	unstable	unstable	unstable
$(0,i_2)$	–	l.a.s.	l.a.s.	l.a.s.	g.a.s.
$(K_-,0)$	unstable	unstable	unstable	unstable	unstable
$(K_+,0)$	l.a.s.	l.a.s.	l.a.s.	unstable	unstable
(P_{3-},i_{3-})	–	–	unstable	unstable	–
(P_{3+},i_{3+})	–	–	–	l.a.s.	–
	extinction			extinction	extinction
	disease-free			endemic	

The left column contains the stationary states (P^*, i^*). The other columns are divided according to the parameter regions along the ray for $\sigma-\alpha$ which are separated by the values in the top row. (*) The most right column corresponds to the case that additionally the function $\phi(P)$ defined in (A.2) does not achieve a positive maximum in (K_-, K_+). 'l.a.s.' stands for locally asymptotically stable, 'g.a.s.' for globally asymptotically stable, and '–' means that the stationary state does not exist or is not feasible.

Table 2
Results of the stability analysis of the non-spatial system (14), (15) with generalized logistic behaviour (5)–(7)

	$\beta(0)$	$\beta(K)$	$\frac{\alpha\beta(0)}{\alpha-g(0)}$	
				$\sigma-\alpha$
$(0,0)$	unstable	unstable	unstable	unstable
$(0,i_2)$	–	–	unstable	g.a.s.
$(K,0)$	g.a.s.	unstable	unstable	unstable
(P_3,i_3)	–	g.a.s.	g.a.s.	–
	disease-free	endemic		extinction

Allee effect alone and independent of the epidemics. Hence, there is always a stable extinction state with a basin of attraction containing at least $0 \leqslant P < K_-$ in the (P, i) phase plane. The extinction state has an ultimate prevalence of either zero or $i_2 > 0$. Note that the trivial state (0, 0) in the logistic model was always unstable.

Increasing the disease-related parameter combination $\sigma-\alpha$, various dynamical regimes can be observed. Due to the Allee effect, there are two bistable regimes, in which the asymptotic behaviour depends on the initial condition, and one monostable regime. These regimes are summarized in the bottom row of Table 1. They are: (i) population extinction or eradication of the disease, (ii) population extinction or endemicity of the disease, and (iii) disease-induced extinction. The last regime is also observed in the logistic case, cf. Table 2.

A closer look at Table 1 reveals that when $\sigma - \alpha < \beta(0)$, there are two locally stable stationary states (0, 0) and (K_+, 0). For $\beta(0) < \sigma - \alpha$, the disease-induced extinction state (0, i_2) emerges and exchanges stability with the trivial solution. The unstable (saddle node) endemic state (P_{3-}, i_{3-}) also exists when $\beta(K_-) < \sigma - \alpha < \beta(K_+)$. For $\sigma - \alpha > \beta(K_+)$, (0, i_2) is still a locally stable stationary state. (K_+,0) and (K_-, 0) are unstable. Two endemic states can exist together, the unstable one and a stable one (P_{3+}, i_{3+}), wherein P_{3+} is the largest root of the function $\phi(P)$ defined in (A.2) within the range (K_-, K_+). Whenever this root exists, the prevalence is given by $i_{3+} = g(P_{3+})/\alpha$, see (A.1). When $\phi(P)$ does not achieve a positive maximum in the range (K_-, K_+), there are no non-trivial states, and the disease-induced extinction state is globally stable.

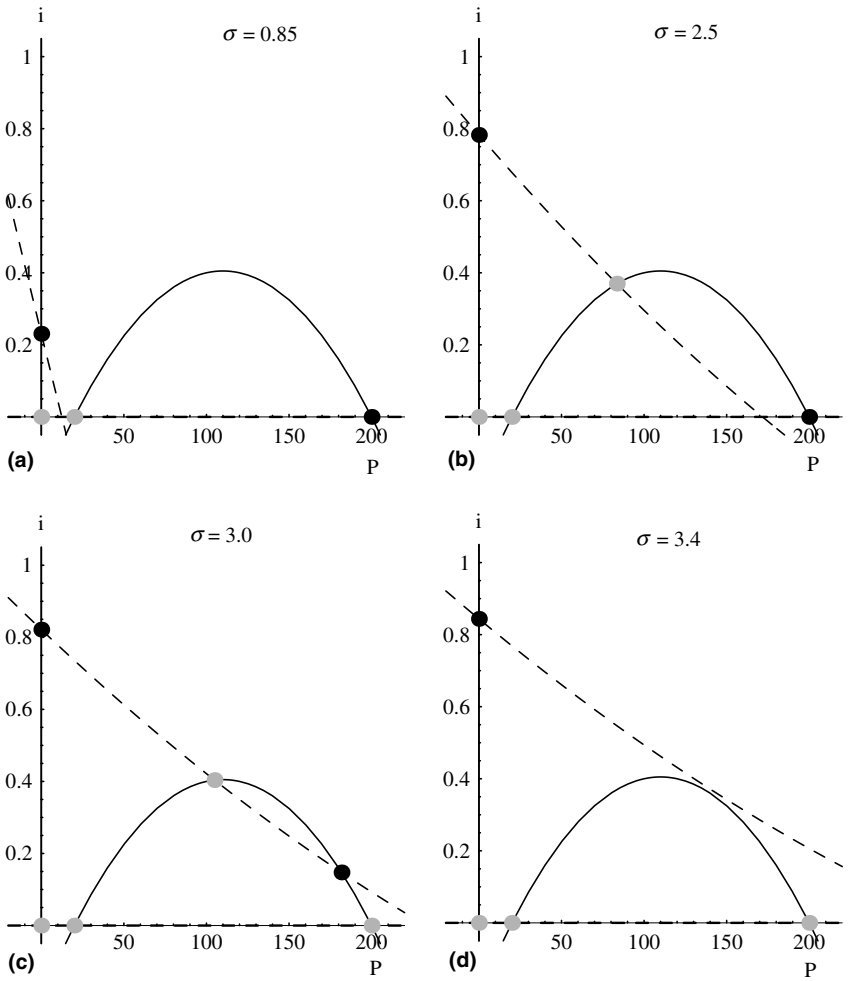

Fig. 2. Nullclines and stationary states in model (14), (15) with Allee effect (12), (13). The solid and the dashed lines are the nullclines of P and i, respectively. Black points are stable equilibria and grey points are unstable equilibria. Other parameter values as in Fig. 1 and $\alpha = 0.2$. Cases (a)–(d) correspond to the four columns from the right-hand side in Table 1.

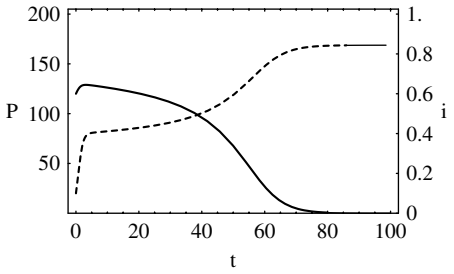

Fig. 3. Transient epidemic in model (14), (15) with Allee effect (12), (13), when the nullclines do not intersect and the disease-induced extinction state is globally stable. The solid and the dashed lines correspond to the course of P and i, respectively. Parameters as in Fig. 2(d), $P(0) = 120$, $i(0) = 0.1$.

It is instructive to consider the nullclines in the phase plane. In Fig. 2, this is done for the motivating example (12), (13). The trivial nullclines are on the axes, while the non-trivial nullclines are quadratics, one open to the bottom and one open to the top. They intersect either in a non-feasible region (a), in a single non-trivial equilibrium (b), in two non-trivial equilibria (c) or in none non-trivial equilibrium (d). Though there is no stationary state in the latter case, the temporal dynamics exhibit a slow-down of the trajectories in the region where the nullclines are close to each other. This results in a 'transient' epidemic, which is shown in Fig. 3.

As noted above, when $0 < P(0) < K_-$, the population dies out by the Allee effect alone. But also for $P(0) > K_-$ numerical simulations show that one may have extinction of the population for a suitable choice of $(P(0), i(0))$. This is a consequence of the joint interplay between the population reduction due to the disease and the Allee effect vital dynamics. While in the model with logistic growth extinction is only possible if $\sigma - \alpha$ is large, the Allee effect generally makes possible the population extinction. Hence, the Allee effect is especially important in the parameter ranges, where the logistic model allows endemicity. In turn, when the dynamics is mainly driven by the losses due to the disease, i.e., $(0, i_2)$ is globally stable, the asymptotic behaviour of the logistic and the Allee model is similar.

4. Spatial spread

Additionally accounting for diffusion as spatial propagation mechanism, this section takes into account the full system (1), (2). Infected individuals are assumed not to be affected by the disease in their mobility, thus $D = D_S = D_I$. Moreover, considerations are restricted to the one-dimensional space, i.e., the Laplacian is set to $\Delta = \partial^2/\partial x^2$. Throughout this section, no-flux boundary conditions are assumed. The initial conditions generally distinguish between a left, middle and right region (which shall later reflect the wake of the host population invasion front in which the disease is introduced, the disease-free invasion front and empty space, respectively):

$$(S(0,x), I(0,x)) = \begin{cases} (S_l, I_l) & \text{if } x < x_l, \\ (S_l, 0) & \text{if } x_l \leqslant x < x_r, \quad 0 < x_l \leqslant x_r. \\ (S_r, 0) & \text{if } x \geqslant x_r, \end{cases} \tag{16}$$

Throughout this paper, S_l will be set to the carrying capacity, i.e. $S_l = K$ for the model with logistic growth and $S_l = K_+$ for the model with Allee effect, and $I_l = 1$. When the host population invades empty space, $S_r = 0$, and if the diseases is introduced into a completely established population, $S_r = S_l$.

For the numerical simulations, the Runge–Kutta scheme of fourth order is applied for the reaction part and an explicit Euler scheme for the diffusion part of the PDE. In order to handle the singularity at the extinction state, a small threshold $\delta = 10^{-10}$ is applied. If $S(t) + I(t) < \delta$, then the transmission terms in (1) and (2) are neglected. In order to suppress effects resulting from a microscopically small band of individuals propagating ahead the actual fronts ('atto-fox problem' [33]), an additional threshold $\epsilon = 10^{-5}$ is applied, below which the population densities of both susceptibles and individuals are simply reset to zero. The value of this threshold has been chosen to weaken atto-effects, but not to change the qualitative behaviour of the waves.

First it should be noted that in the disease-free model ($I = 0$) travelling frontal waves with constant speed and shape emerge [46–49]. There is a minimum wave speed in the model with logistic growth and a unique wave speed in the model with Allee effect, which respectively are

$$v = 2\sqrt{rD}, \tag{17}$$

$$v = \sqrt{2aD}(K_+/2 - K_-). \tag{18}$$

There are two particularities in the Allee effect model.

(1) When the Allee threshold $K_- > K_+/2$, then the population wave moves backward.
(2) Such one-component bistable reaction–diffusion systems are known to show nucleation-type behaviour, i.e., nucleii of a stable 'phase' $P = K_+$ in an unstable phase $P = 0$ will decay unless they have reached a certain critical size, cf. [50–52]. Otherwise, they advance with the asymptotic rate of spread given in (18).

4.1. Spread in a settled disease-free population

The situation is considered that the disease-free population has established in all the space at carrying capacity, i.e. $S_r = K$ or $S_r = K_+$, respectively, and that infected individuals are at the left-hand boundary as specified in (16).

The numerical simulation of the model with logistic growth is shown in Fig. 4. A travelling infection wave emerges and advances with a constant speed v. In its wake, the population settles down to the endemic state. The infection front propagates with a speed of $v = 1.2$ km/year. This matches well the wave speed which can also be easily derived by linearization of the equations 'at the leading edge', i.e., far in front of the travelling front where $S \approx K$ and $I \approx 0$. Then the equation for I in (1), (2) reduces to be of Skellam/Luther type [53,54], and the minimum wave speed is

$$v = 2\sqrt{(\sigma - \alpha - b)D}. \tag{19}$$

In the model with Allee effect, the emergence and propagation of a travelling wave can be observed, too. With the same approach as above, one obtains the wave speed

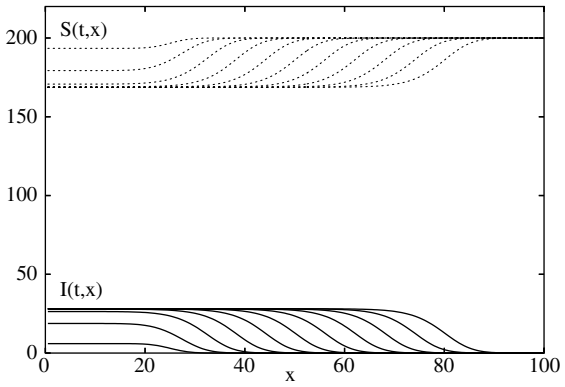

Fig. 4. Travelling infection wave in the SI model with logistic growth (3,4). The solid lines represent I, the dashed lines S. Displayed are different snapshots, which have been taken in a time interval with a delay of 5, beginning at $t = 5$ and ending at $t = 55$ (from left to right). Parameters as in Fig. 1(a), $\sigma = 3.0$, $\alpha = 0.2$, $S_r = K$, $x_l = x_r = 5$.

$$v = 2\sqrt{(\sigma - \alpha - a[c + (e + K_-)K_+])D}. \tag{20}$$

This is an approximation and has to be taken with caution, because the travelling front in the Allee effect model is a 'pushed' wave. Because the infection spreads within a population which has established at carrying capacity, we argue that (20) may be a reasonable approximation provided that the coexistence state is large enough and, thus, the total population is throughout the travelling wave quite far away from small densities which might cause significant impacts due to the Allee effect. In order to check the robustness of (20) against P_{3+}, numerical simulations were run with varying transmission coefficient σ. The results in Fig. 5 show a very good accordance. However, we want to emphasize that in other parameter ranges where P_{3+} is closer to the Allee threshold regions the match possibly might not be as good.

Both wave speed approximations include the disease-related parameters and the diffusivity. In the model with logistic growth, only the birth rate is additionally included. This reflects that the

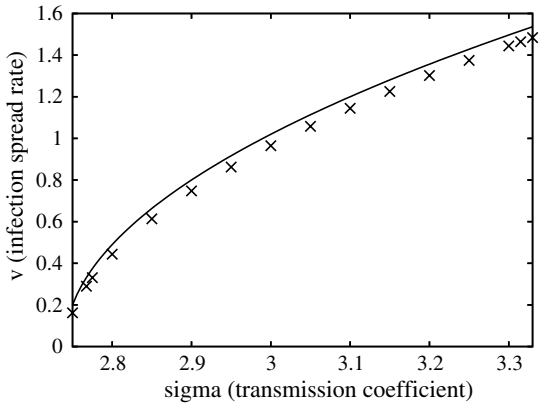

Fig. 5. Wave speed of disease spread in an established host population with Allee effect. The line is the approximation (20) and the data points are numerical results. Parameter values as in Fig. 1 with $\alpha = 0.2$. The values for the transmission coefficient σ have been chosen according to the existence of the endemic state (P_{3+}, i_{3+}).

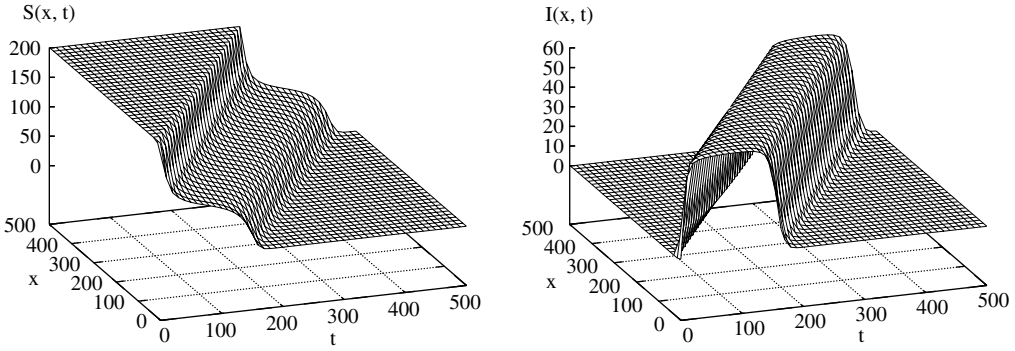

Fig. 6. Travelling fatal epidemic with succeeding host population extinction. Model with Allee effect, parameter values as in Fig. 2(d), $S_r = K_+$, $x_l = x_r = 10$.

wave is 'pulled', whereas the Allee effect-wave is 'pushed', and therefore also the other vital parameters play a role, e.g., the Allee threshold and the carrying capacity.

Next, if the transmission coefficient is further increased than in Fig. 5, the non-trivial states disappear and the disease-induced extinction state $(0, i_2)$ is globally stable, cf. Table 1. Numerical simulations show the propagation of travelling pulse-like epidemics that wipe out the host population as displayed in Fig. 6. This effect is a result of the 'transient' epidemic, cf. Fig. 3. The length of the pulse depends on how closely the non-trivial nullclines approach each other (Fig. 2(d)). The travelling epidemic with succeeding population extinction is associated with the stability of the disease-induced extinction state. Hence, this fatal epidemic wave can also be obtained in the model with logistic growth if the parameters are appropriately chosen, cf. Table 2.

4.2. Spread in colonizing population

Now, the host population is assumed still to be in a colonizing process, i.e. $S_r = 0$. The disease is subsequently introduced in the wake of the host population front, cf. (16).

In the logistic SI model with the FIV parameters, the speed (17) of the invading host population is larger than the speed (19) of the disease. Thus, the distance between the two fronts increases with time. However, the infection wave can catch up the disease-free front, if $\sigma - \alpha > 2b - m$. This is illustrated in Fig. 7. For a better visualization, the waves are now displayed in the (x, t) plane with a grey colour shading according to the densities of susceptibles and infected. The infection and the host population invasion front combine to a travelling front of the endemic state into empty space. The numerical results show that this front moves with the same speed (17) as the invading host population. This means that the infection spread rate is reduced to this speed, because of which there is a kink in the expansion of I in Fig. 7.

In the model with Allee effect, three different types of spatiotemporal dynamics can be observed when a catch-up has taken place. First, the endemic front does not move with the same speed (18) as the disease-free invasion front before. Instead, the endemic front either slows down or becomes recessive. The latter case of front reversal is shown in Fig. 8. Shortly before the catchup, the remaining 'atto-individuals' cause a hump of infection ahead of the actual infection front. Then, there is a retreat of the total population, which corresponds to a wave of extinction, though the

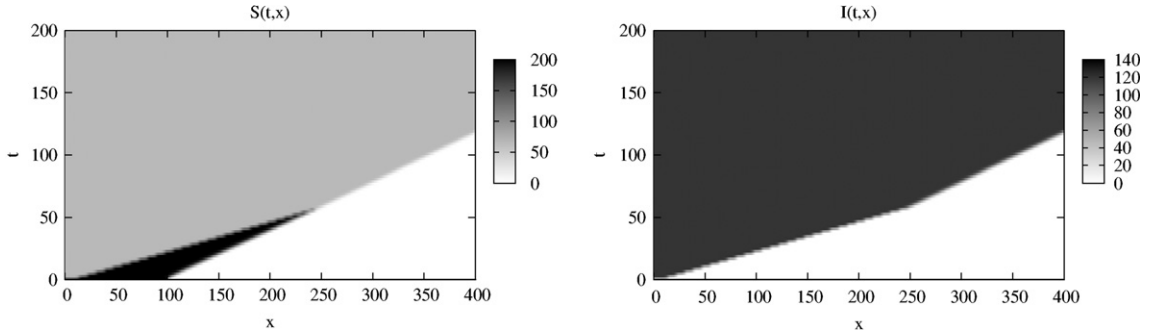

Fig. 7. Travelling infection wave introduced in the wake of an invading host population with logistic growth. When the disease catches up the invading host population front, the disease spread is slowed down, but the host population (now endemic) still advances with the same speed. Parameters as in Fig. 4, but with $S_r = 0$, $x_l = 5$, $x_r = 100$ and $\sigma = 7$, in order to enable the catch-up.

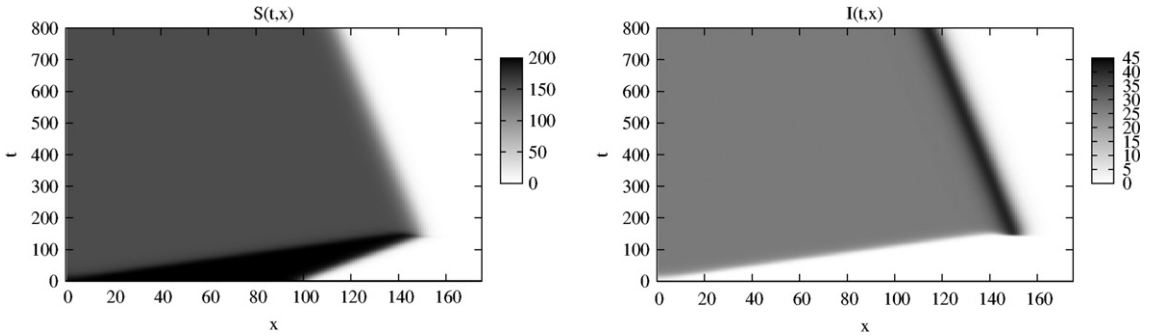

Fig. 8. Front reversal in the model with Allee effect, when the infected front catches up the host population front. Parameters as in Fig. 2(c) with $S_r = 0$, $x_l = 5$, $x_r = 100$.

coexistence state is locally stable. Note the increased density of infected at the head of the retreating front. A detailed study of this phenomenon is given in [25].

Second, when there is a unique, unstable non-trivial equilibrium as in Fig. 2(b), a travelling infection pulse emerges, which propagates jointly with the front of the host population. This corresponds to a travelling epidemic and is illustrated in Fig. 9. Though the infection pulse continues its advancement as long as there are no boundary restrictions, the disease fades out at a fixed location in space when the pulse has passed. Then, the population approaches the carrying capacity again – in contrast to the fatal epidemic with succeeding population extinction shown in Fig. 6. It should be noted, that the emergence of this travelling pulse requires appropriate values of σ, initial conditions as well as x_l and x_r being close enough to each other.

Third, consider the parameter region where the disease-induced extinction state is globally stable and a transient epidemic develops as in Fig. 3. Then the disease-free population spreads in an invasion front, and the introduced disease causes a travelling epidemic before the ultimate extinction due to the transient dynamics, cf. Fig. 10. Thus far this effect is the same as the fatal epidemic (Fig. 6). The finite initial distribution of the host population, however, induces the disappearance

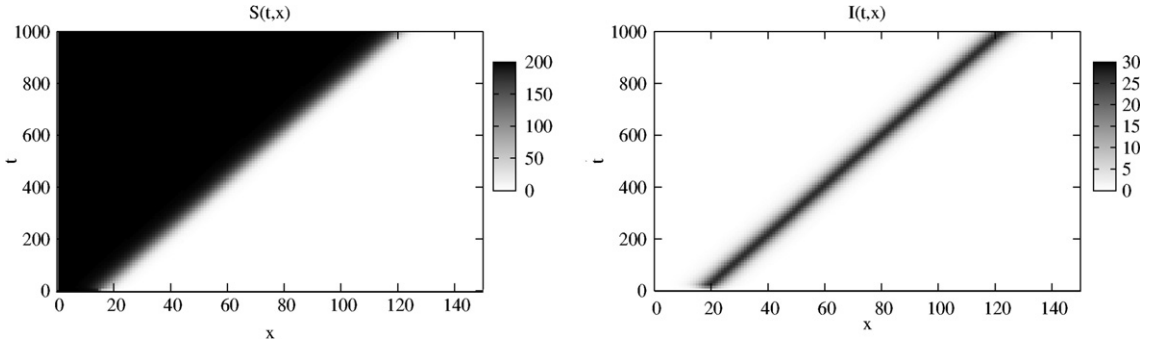

Fig. 9. Infection pulse in the model with Allee effect. Parameters as in Fig. 8, except $\sigma = 2.5$ and $x_l = 10$, $x_r = 15$.

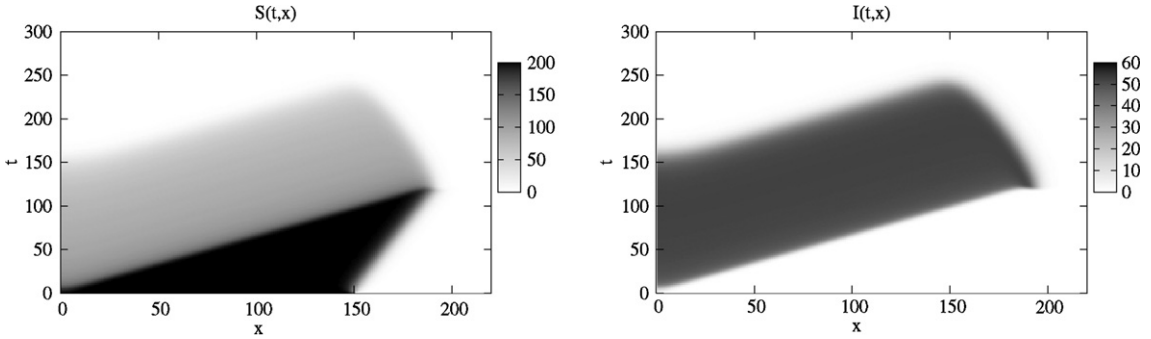

Fig. 10. Spatially restricted epidemic in the model with Allee effect. In the non-spatial model, there is no non-trivial state and the disease-induced extinction state is globally stable. Parameters as in Fig. 8, except $\sigma = 3.4$, what yields the local dynamics as in Fig. 3. $x_l = 5$, $x_r = 150$.

of the epidemic wave. When the infection catches up the invading host population, there is again a front reversal of the endemic state, and thus a travelling wave of extinction limits the propagation of the epidemics. This results in the spatial extinction of the total population, and the epidemic could only spread within a spatially restricted area. Note that this effect is also possible in the model with logistic growth since it is associated with the disease-induced extinction state as well as appropriate initial conditions.

5. Discussion and conclusions

This paper has investigated the impact of a strong Allee effect in the vital dynamics of an epidemiological SI model upon the temporal and spatiotemporal disease spread as well as on the host population. First of all, the Allee effect induces a threshold value in the initial conditions below which the population dies out (minimum viable population size) and a critical value of the spatial length of an initial nucleus (also called the problem of critical aggregation, cf. [55]). Numerical simulations show that both phenomena are strengthened in the presence of the disease.

Furthermore, the Allee effect leads to bistability in the local transmission dynamics. Jointly with the minimum viable population size, this has severe implications for possible control methods, since they do not necessarily rely on reducing the basic reproductive ratio anymore. Instead, disease control could be established by shifting the system's trajectory in the desired domain of attraction, which may be easier to manage than modifying parameter regimes.

If the infectiousness of the disease, i.e., a high transmissibility and/or a small enough virulence, is large in comparison with the demographic reproductiveness, the Allee effect becomes less important, because the population dynamics is dominantly driven by the disease to extinction. This disease-induced extinction state is typical for epidemiological models with proportionate mixing transmission and has also been found in models with vital dynamics of logistic, exponential or recruitment type. Similarly, sustained oscillations could not be found in the model with Allee effect, either. There are, however, three other additional features: (i) The trivial state can be locally stable. (ii) There is a second non-trivial state, which is always unstable. (iii) In the parameter range of disease-induced extinction, there is still an epidemic possible, if the non-trivial nullclines are close to each other. The importance of transient dynamics has recently been highlighted in [56].

The emergence and propagation of travelling frontal waves of infection have been numerically observed in a spatial setting. Analytical wave speed approximations have been derived for the cases when the disease propagates in an established host population. When the host population itself still colonizes empty space, various spatiotemporal dynamics can be observed. In the model with logistic growth the infection front is slowed down to the constant invasion speed of the host population, which is not affected by this catch-up. In contrast, in the model with Allee effect, the propagation of the host population front is either slowed down or reversed. Thus, the extinction of the invasive host population is possible when the disease is subsequently introduced. This is a mechanism which can be attributed to the joint interplay of the Allee effect, the disease and the spatial diffusion. Thus, the virus might be a potential biocontrol agent, cf. [57]. A similar dynamics has been observed in predator-prey models in which the prey exhibits an Allee effect [58,59]. An analytical investigation of this effect is challenging because of the set of two PDEs with cubic nonlinearity, but possible approaches are presented in [25]. Pathogen-driven host extinction in a spatial context has also been observed in a model of lattice structured populations [60,61].

Moreover, travelling infection pulses in front of the colonizing host population can be observed if the unique endemic state is unstable in the local dynamics. This is an additional feature of the model with Allee effect. Both models with Allee effect and logistic growth can exhibit travelling fatal epidemics with host extinction in the parameter regime with the 'transient' epidemic. This is associated with the globally stable disease-induced extinction state. If the initial distribution of the host population is finite, a spatially restricted infection front appears before ultimate population extinction.

Overall, the Allee effect induces a rich variety of (spatio-)temporal dynamics in the considered epidemiological model. Since it can have significant consequences on the fate of epidemics, endemics and invasions, its role has to be further investigated. Of particular interest would be the robustness of the current results against other epidemiological details such as transmission functions, vertical transmission or disease-related reduced fertility. The extension of an exposed compartment, for instance, enables sustained oscillations if disease transmission is of mass action type [19]. Recent results indicate that the Allee effect makes possible limit cycle oscillations in an

SI model with mass action transmission (Hilker et al., in prep.), even if there is no exposed compartment.

Acknowledgments

The authors thank two anonymous reviewers for their comments which helped improving the paper. This work was initiated in February 1996 while M.L. was holding a visiting position at Kyushu University under a grant from the Japan Society for the Promotions of Science (JSPS). S.P. acknowledges partial support from the University of California Agricultural Experiment Station through Professor Bai-Lian Li.

Appendix A. Stability analysis of the non-spatial model

We consider the ODE system (14), (15) with the assumptions (8)–(11) for a generalized strong Allee effect. For the sake of simplicity, let the prime denote differentiation with respect to P. We will apply this notation to $g(P)$, $\beta(P)$ and $\phi(P)$.

One may check that the domain $P \geqslant 0$ and $0 \leqslant i \leqslant 1$ is invariant; moreover, no trajectory starting at $P(t=0) > 0$ and $i(t=0) > 0$ may hit the boundary $P = 0$ or the boundary $i = 0$ in finite time. There are four (semi-)trivial stationary states:

- $P_0 = 0$ and $i_0 = 0$,
- $P_{1+} = K_+$ and $i_{1+} = 0$,
- $P_{1-} = K_-$ and $i_{1-} = 0$,
- $P_2 = 0$ and $i_2 = [\sigma - \alpha - \beta(0)]/(\sigma - \alpha)$; it is feasible, i.e., $0 < i_2 \leqslant 1$, if and only if $\sigma - \alpha > \beta(0)$.

Looking for a non-trivial stationary state with $0 < P_3 \leqslant K_+$ and $0 < i_3 \leqslant 1$ one finds

$$i_3 = \frac{g(P_3)}{\alpha} = \frac{\sigma - \alpha - \beta(P_3)}{\sigma - \alpha}. \tag{A.1}$$

Thus, a necessary condition to have a non-trivial stationary state is $\sigma - \alpha > 0$. Introducing the function $\phi(P)$ defined as

$$\phi(P) = (\sigma - \alpha)g(P) + \alpha\beta(P) - \alpha(\sigma - \alpha),$$

one is left with finding P_3 as a root of

$$\phi(P_3) = 0 \quad \text{in } (K_-, K_+), \tag{A.2}$$

because, by (8), (9), $g(P)$ is non-positive in $(0, K_-)$. Still assuming $\sigma - \alpha > 0$, from conditions (10) and (11), $\phi(P)$ is concave in this range; hence there are either 0, 1 or 2 feasible roots. Let us denote P_{3-} the root located on the increasing branch of ϕ and P_{3+} the root located on the decreasing branch of ϕ, when such roots exist. In order to be a little bit more precise, let us recall that $g(0) < 0$ and $g(K_-) = g(K_+) = 0$; thus, using the monotonicity of the death-rate $\mu(P)$, it follows

$$0 \leqslant \beta(0) < \beta(K_-) \leqslant \beta(K_+) \quad \text{and} \quad \phi(K_-) \leqslant \phi(K_+).$$

Hence, still assuming $\sigma - \alpha > 0$, one has

(1) no non-trivial stationary solution when $\phi(K_-) \geqslant 0$, say $0 < \sigma - \alpha \leqslant \beta(K_-)$;
(2) a unique non-trivial stationary solution (P_{3-}, i_{3-}), when $\phi(K_-) < 0 \leqslant \phi(K_+)$, say $\beta(K_-) < \sigma - \alpha \leqslant \beta(K_+)$;
(3) two non-trivial stationary solutions, labelled (P_{3-}, i_{3-}) and (P_{3+}, i_{3+}), or
(4) none when $\phi(K_-) \leqslant \phi(K_+) < 0$, say $\beta(K_-) \leqslant \beta(K_+) < \sigma - \alpha$; this depends on whether ϕ achieves a positive maximum in (K_-, K_+) or not.

This is illustrated in Fig. 11. It should be noted that $g'(P_{3+}) < 0$: assuming the opposite yields $\beta'(P_{3+}) > 0$ and therefore $\phi'(P_{3+}) > 0$, a contradiction.

The local stability analysis of the (semi-)trivial stationary states follows from the computation of the Jacobian matrix that is either a diagonal or a triangular matrix. The results are summarized in Table 1. Finally, at any non-trivial stationary state

$$J(P_3, i_3) = \begin{pmatrix} g'(P_3)P_3 & -\alpha P_3 \\ -\beta'(P_3)i_3 & -(\sigma - \alpha)i_3 \end{pmatrix}.$$

One has $\phi'(P_{3+}) < 0$, so that the determinant of $J(P_{3+}, i_{3+})$ is positive; its trace is negative because as noted above $g'(P_{3+}) < 0$ and $\sigma - \alpha > 0$ as soon as P_{3+} is feasible, yielding the local stability of (P_{3+}, i_{3+}) as soon as it is feasible. Conversely, $\det J(i_3, P_3) = -i_3 P_3 \phi'(P_3)$ so that (P_{3-}, i_{3-}) is unstable when it is feasible because $\phi'(P_{3-}) > 0$. To be more precise, (P_{3-}, i_{3-}) is always a saddle. Using this fact, we obtain from index theory that there cannot be any limit cycles. The index theory can give insight into the qualitative behaviour of closed orbits and multiple equilibria of planar dynamical systems [9,62]. In particular, the index of any simple closed curve is equal to the sum of the indices of all equilibria in the interior of the curve. The index of a periodic orbit is +1. Within the positive interior, there exist either only (P_{3-}, i_{3-}) that is always a saddle with index −1 or also (P_{3+}, i_{3+}) that is always stable with index +1. Hence, there cannot be any periodic orbit – neither around (P_{3-}, i_{3-}) nor around both (P_{3-}, i_{3-}) and (P_{3+}, i_{3+}). Note that a homoclinic orbit should not be treated as a periodic orbit for the application of index theory [62], because of which we restrict or conclusion to the non-existence of limit cycle oscillations.

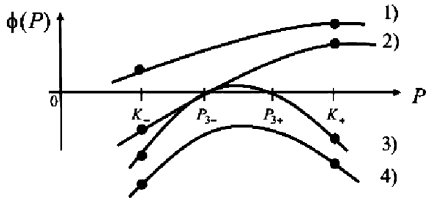

Fig. 11. The number of non-trivial stationary states in model (14), (15) with Allee effect (12), (13) depends on the location of $\phi(P)$. Four different cases are possible. Their numbering refers to the description in the text.

References

[1] N. Shigesada, K. Kawasaki, Biological Invasions: Theory and Practice, Oxford University, Oxford, 1997.
[2] O. Diekmann, J.A.P. Heesterbeek, Mathematical Epidemiology of Infectious Diseases, Model Building, Analysis and Interpretation, Wiley, New York, 2000.
[3] J.D. Murray, Mathematical Biology. I: An Introduction, third ed., Springer, Berlin, 2002.
[4] J.D. Murray, Mathematical Biology. II: Spatial Models and Biomedical Applications, third ed., Springer, Berlin, 2003.
[5] R.S. Cantrell, C. Cosner, Spatial Ecology via Reaction–Diffusion Equations, Wiley, Chichester, 2003.
[6] H.R. Thieme, Mathematics in Population Biology, Princeton University, Princeton, NJ, 2003.
[7] W.O. Kermack, A.G. McKendrick, Contribution to the mathematical theory of epidemics, part I, Proc. Roy. Soc. A 115 (1927) 700.
[8] W.O. Kermack, A.G. McKendrick, Contribution to the mathematical theory of epidemics. II – The problem of endemicity, Proc. Roy. Soc. A 138 (1932) 55.
[9] F. Brauer, C. Castillo-Chavez, Mathematical Models in Population Biology and Epidemiology, Springer, New York, 2001.
[10] R.M. Anderson, R.M. May, Population biology of infectious diseases: Part I, Nature 280 (1979) 361.
[11] F. Brauer, Models for the spread of universally fatal diseases, J. Math. Biol. 28 (1990) 451.
[12] S. Busenberg, P. van den Driessche, Analysis of a disease transmission model in a population with varying size, J. Math. Biol. 28 (1990) 257.
[13] A. Pugliese, Population models for diseases with no recovery, J. Math. Biol. 28 (1990) 65.
[14] O. Diekmann, M. Kretzschmar, Patterns in the effects of infectious diseases on population growth, J. Math. Biol. 29 (1991) 539.
[15] L.Q. Gao, H.W. Hethcote, Disease transmission models with density-dependent demographics, J. Math. Biol. 30 (1992) 717.
[16] J. Mena-Lorca, H.W. Hethcote, Dynamic models of infectious diseases as regulator of population sizes, J. Math. Biol. 30 (1992) 693.
[17] J. Zhou, H.W. Hethcote, Population size dependent incidence in models for diseases without immunity, J. Math. Biol. 32 (1994) 809.
[18] D. Greenhalgh, R. Das, Modelling epidemics with variable contact rates, Theor. Populat. Biol. 47 (1995) 129.
[19] R.M. Anderson, H.C. Jackson, R.M. May, A.M. Smith, Population dynamics of foxes rabies in Europe, Nature 289 (1981) 765.
[20] F. Courchamp, D. Pontier, M. Langlais, M. Artois, Population dynamics of Feline Immunodeficiency Virus within cat populations, J. Theor. Biol. 175 (4) (1995) 553.
[21] B. Dennis, Allee effects: population growth, critical density, and the chance of extinction, Natural Resour. Model. 3 (1989) 481.
[22] F. Courchamp, T. Clutton-Brock, B. Grenfell, Inverse density dependence and the Allee effect, Trends Ecol. Evolut. 14 (10) (1999) 405.
[23] P.A. Stephens, W.J. Sutherland, R.P. Freckleton, What is the Allee effect? Oikos 87 (1) (1999) 185.
[24] P.A. Stephens, W.J. Sutherland, Consequences of the Allee effect for behaviour, ecology and conservation, Trends Ecol. Evolut. 14 (10) (1999) 401.
[25] F.M. Hilker, M.A. Lewis, H. Seno, M. Langlais, H. Malchow, Pathogens can slow down or reverse invasion fronts of their hosts, Biol. Invas. 7 (5) (2005) 817.
[26] S.V. Petrovskii, H. Malchow, F.M. Hilker, E. Venturino, Patterns of patchy spread in deterministic and stochastic models of biological invasion and biological control, Biol. Invas. 7 (2005) 771.
[27] J.V. Noble, Geographic and temporal development of plagues, Nature 250 (1974) 726.
[28] D. Mollison, Spatial contact models for ecological and epidemics spread, J. Roy. Statist. Soc. B 39 (3) (1977) 283.
[29] J.D. Murray, E.A. Stanley, D.L. Brown, On the spatial spread of rabies among foxes, Proc. Roy. Soc. Lond. B 229 (1986) 111.
[30] A. Okubo, P.K. Maini, M.H. Williamson, J.D. Murray, On the spatial spread of the gray squirrel in Britain, Proc. Roy. Soc. Lond. B 238 (1989) 113.

[31] S. Yachi, K. Kawasaki, N. Shigesada, E. Teramoto, Spatial patterns of propagating waves of fox rabies, Forma 4 (1989) 3.
[32] F. van den Bosch, J.A.J. Metz, O. Diekmann, The velocity of spatial population expansion, J. Math. Biol. 28 (1990) 529.
[33] D. Mollison, Dependence of epidemics and populations velocities on basic parameters, Math. Biosci. 107 (1991) 255.
[34] G. Dwyer, Density dependence and spatial structure in the dynamics of insect pathogens, Amer. Naturalist 143 (4) (1994) 533.
[35] T. Caraco, S. Glavanakov, G. Chen, J.E. Flaherty, T.K. Ohsumi, B.K. Szymanski, Stage-structured infection transmission and a spatial epidemic: a model for lyme disease, Amer. Naturalist 160 (3) (2002) 348.
[36] G. Abramson, V.M. Kenkre, T.L. Yates, R.R. Parmenter, Traveling waves of infection in the hantavirus epidemics, Bull. Math. Biol. 65 (2003) 519.
[37] L. Rass, J. Radcliff, Spatial Deterministic Epidemics, American Mathematical Society, Providence, RI, 2003.
[38] F. Courchamp, G. Sugihara, Modeling the biological control of an alien predator to protect island species from extinction, Ecol. Appl. 9 (1) (1999) 112.
[39] F. Courchamp, S.J. Cornell, Virus-vectored immunocontraception to control feral cats on islands: a mathematical model, J. Appl. Ecol. 37 (2000) 903.
[40] A. Nold, Heterogeneity in disease-transmission modeling, Math. Biosci. 52 (1980) 227.
[41] H.W. Hethcote, The mathematics of infectious diseases, SIAM Rev. 42 (4) (2000) 599.
[42] H. McCallum, N. Barlow, J. Hone, How should pathogen transmission be modelled? Trends Ecol. Evolut. 16 (6) (2001) 295.
[43] E. Fromont, D. Pontier, M. Langlais, Dynamics of a feline retrovirus (FeLV) in host populations with variable spatial structure, Proc. Roy. Soc. Lond. B 265 (1998) 1097.
[44] E. Fromont, D. Pontier, M. Langlais, Disease propagation in connected host populations with density-dependent dynamics: the case of the Feline Leukemia Virus, J. Theor. Biol. 223 (2003) 465.
[45] F. de Castro, B. Bolker, Mechanisms of disease-induced extinction, Ecol. Lett. 8 (2005) 117.
[46] R.A. Fisher, The wave of advance of advantageous genes, Ann. Eugenics 7 (1937) 355.
[47] A.N. Kolmogorov, I.G. Petrovskii, N.S. Piskunov, Étude de l'equation de la diffusion avec croissance de la quantité de matière et son application à un problème biologique, Bulletin Université d'Etat à Moscou, Série internationale, section A 1 (1937) 1.
[48] D.G. Aronson, H.F. Weinberger, Nonlinear diffusion in population genetics, combustion, and nerve propagation, in: J.A. Goldstein (Ed.), Partial Differential Equations and Related Topics, no. 446 in Lecture Notes in Mathematics, Springer, Berlin, 1975, p. 5.
[49] M.A. Lewis, P. Kareiva, Allee dynamics and the spread of invading organisms, Theor. Populat. Biol. 43 (1993) 141.
[50] A. Nitzan, P. Ortoleva, J. Ross, Nucleation in systems with multiple stationary states, Faraday Symp. Chem. Soc. 9 (1974) 241.
[51] H. Malchow, L. Schimansky-Geier, Noise and diffusion in bistable nonequilibrium systems, no. 5 in Teubner-Texte zur Physik, Teubner-Verlag, Leipzig, 1985.
[52] W. van Saarlos, Front propagation into unstable states, Phys. Rep. 386 (2003) 29.
[53] J.G. Skellam, Random dispersal in theoretical populations, Biometrika 38 (1951) 196.
[54] R. Luther, Räumliche Ausbreitung chemischer Reaktionen, Z. Elektrochem. 12 (1906) 596.
[55] S. Petrovskii, N. Shigesada, Some exact solutions of a generalized Fisher equation related to the problem of biological invasion, Math. Biosci. 172 (2001) 73.
[56] A. Hastings, Transients: the key to long-term ecological understanding? Trends Ecol. Evolut. 19 (2004) 39.
[57] W.F. Fagan, M.A. Lewis, M.G. Neubert, P. van den Driessche, Invasion theory and biological control, Ecol. Lett. 5 (2002) 148.
[58] M.R. Owen, M.A. Lewis, How predation can slow, stop or reverse a prey invasion, Bull. Math. Biol. 63 (2001) 655.
[59] S.V. Petrovskii, H. Malchow, B.-L. Li, An exact solution of a diffusive predator–prey system, Proc. Roy. Soc. Lond. A 461 (2005) 1029.

[60] K. Sato, H. Matsuda, A. Sasaki, Pathogen invasion and host extinction in lattice structured populations, J. Math. Biol. 32 (1994) 251.
[61] Y. Haraguchi, A. Sasaki, The evolution of parasite virulence and transmission rate in a spatially structured population, J. Theor. Biol. 203 (2000) 85.
[62] S. Wiggins, Introduction to Applied Nonlinear Dynamical Systems and Chaos, second ed., Springer, New York, 2003.